Microstructure and electrical properties of $SrTi_{0.98}Nd_{0.02}O_{3-\delta}$-based composites applied as porous layers for SOFCs[#]

Beata Bochentyn, Bogusław Kusz

Department of Solid State Physics, Gdansk University of Technology, ul. Narutowicza 11/12, 80-233 Gdansk, Poland

Received 27 October 2011; received in revised form 20 February 2012; accepted 25 February 2012

Abstract

$SrTi_{0.98}Nb_{0.02}O_{3-\delta}$-$CeO_2$ and $SrTi_{0.98}Nb_{0.02}O_{3-\delta}$-YSZ composites have been prepared. In order to evaluate the applicability of the material for solid oxide fuel cells (SOFCs) both bulk samples and porous composite layers have been investigated. The electrical conductivity of the bulk samples was measured using the four-terminal DC method, whereas the conductivity of the porous layers was determined using the DC Van der Pauw method in the temperature range of 400–850 °C in humidified hydrogen. The microstructure of the samples was characterized by scanning electron microscopy (SEM) technique. From the fuel cells point of view a significant advantage of the bulk $Sr(Ti,Nb)O_{3-\delta}$-YSZ over $Sr(Ti,Nb)O_{3-\delta}$-CeO_2 composite was noticed in the case of microstructure and electrical properties. Ceria grains in the $Sr(Ti,Nb)O_{3-\delta}$-CeO_2 composite tend to form large clusters, especially at the grain boundaries. This phenomenon results in sample cracking during redox cycles.

Keywords*: solid oxide fuel cell, anode, composite, microstructure*

I. Introduction

Solid oxide fuel cell (SOFC) is a promising device that directly converts the chemical energy of various gaseous fuels into electrical energy and heat. It consists of essentially four components: electrolyte, cathode, anode and interconnect. The most often used anode for SOFCs is a Ni-YSZ (metallic-ceramic) composite of NiO and YSZ called nickel cermet. It has many advantages, such as catalytic activity, thermal expansion coefficient (TEC) compatible with the electrolyte (YSZ) [1] and very high value of electrical conductivity [2]. However, it is also sensitive to deposition of carbon on the electrode, which blocks the anode reaction and can be poisoned by sulphur [2,3]. Such problems limit the possibility of using Ni-YSZ for carbon-containing fuels. Moreover, Ni-YSZ can undergo microstructural changes during redox cycles, which can reduce the three-phase area and thereby reduce the electrode activity [2,3]. Hence, it is necessary to investigate some alternative materials, such as perovskite-related structures. Among them $SrTiO_3$ is one of the most promising compositions, but in a pure form it is a dielectric material. Its electronic conductivity can be increased simply by high temperature reduction and substituting with some donor dopants [4–7]. However, its ionic conductivity and electrocatalytic activity are still too low for commercial application of this material [8]. Moreover, there is a mechanical misfit between pure strontium titanate and yttria-stabilized zirconia (YSZ) electrolyte. This indicates the need to use composite materials to make the operating fuel cell more efficient and mechanically stronger [9–11]. The most popular are the composites consisting of the electrolyte and anode material. The former component is ionic conductor, whereas the later is an electronic conductor. Material prepared in this way prevents the process of layers delamination and increases the triple phase boundary (TPB), which should result in the improved performance of the fuel cell. Also, composites with some catalysts can be prepared in order to increase the electrocatalytic activity of the material.

The aim of this work is to discuss microstructure and electrical properties of composites consisting of

[#] Paper presented at *Conference for Young Scientists - 9th Students' Meeting, SM-2011,* Novi Sad, Serbia, 2011

* Corresponding author: tel: +48 58 347 23 32
fax: +48 58 347 28 21, e-mail: *bbochentyn@mif.pg.gda.pl*

$SrTi_{0.98}Nb_{0.02}O_{3-\delta}$ and CeO_2 or YSZ. In order to evaluate the applicability of the materials, both bulk samples and porous composite layers are investigated.

II. Experimental

The ceramic $SrTi_{0.98}Nb_{0.02}O_{3-\delta}$ (further denoted as STNb2) powder was prepared using a conventional solid-state reaction method reported elsewhere [5]. An optimal amount of Nb is 2 mol%, as it gives the highest conductivity in comparison with the other investigated compositions [5]. The fine-grained $SrTi_{0.98}Nb_{0.02}O_{3-\delta}$ powder was mixed in proper weight ratio with YSZ (8 mol% yttria-stabilized zirconia, Daiichi Kigenso HSY-8) or with CeO_2 (Fluka) powders in a ball mill for 12 h to obtain well dispersed powder mixtures. Latter in the paper these composites will be denoted as *x*STNb2-(1-*x*)YSZ and *x*STNb2-(1-*x*)CeO_2, where x = 70 or 85 wt.% of STNb2 which correspond to 73 and 87 vol.% of STNb2 in the case of STNb2-YSZ composites and to 77 and 89 vol.% of STNb2 in the case of STNb2-CeO_2.

The investigations were performed on both bulk samples and porous composite layers (thick films). The bulk samples were prepared by uniaxial pressing and sintering of the pressed pellets at 1400 °C for 10 h in H_2. To obtain suitable porosity the composite powder was mixed with starch (5 wt.%). Layers were prepared by mixing the composite powder with an organic binder ESL403, and the resulting paste was deposited onto the surface of the YSZ electrolyte foil (thickness ~150 μm) forming the so-called half-cell. Before painting the paste onto the foils, the foils were appropriately cut and sintered at 1400 °C. In order to burn out the organic binder, the thick film samples were calcined at 700 °C for 3 h in air. To improve the electrical properties of the prepared compounds they were reduced in dry hydrogen at 1400 °C for 10 h.

The composites were examined using various methods. The electrical conductivity of the bulk samples was measured using the four-terminal DC method over the temperature range of 400–950 °C in humidified hydrogen. The measurements were

performed at constant heating and cooling rates (2 °C/min) on ground bar samples with parallel 9907 ESL silver electrodes. The conductivity of the porous layers was determined using the DC Van der Pauw method in the temperature range of 400–850 °C. To ensure that the measurements were performed at equilibrium conditions, the samples were held at each temperature for over 60 minutes before the measurement was made. The morphology of the samples was characterized in the Hitachi TM3000 scanning electron microscope (SEM), using secondary electron (SE) detector. To recognize the elements on the composite surface the energy-dispersive X-ray spectroscopy (EDX) was performed by the Bruker AXS Quantax 200 spectrometer in particular area of the sample.

III. Results and discussion

The results of XRD investigations of the STNb2-YSZ and STNb2-CeO_2 composites have been performed and reported in our previous paper [12]. They indicate that all of the reflections observed in XRD patterns can be attributed to either strontium titanate or YSZ/CeO_2 phases and in the range of equipment sensitivity no sign of reaction between phases can be found.

The cross-sections of the composite bulk samples reduced at 1400 °C for 10 h in H_2 are presented in Fig. 1. It can be seen that in the 70STNb2-30CeO_2 sample (Fig. 1a) the large (5 μm) grains are separated from each other by smaller CeO_2 (1–2 μm) crystallites, whereas in the 70STNb2-30YSZ composite (Fig. 1b) a fine-crystalline YSZ phase is well dispersed among larger grains of STNb2 phase. This can explain our observations of macrostructure performed at the reduced composites, namely the cracking of both the bulk samples and the composite layers containing ceria during the process of high

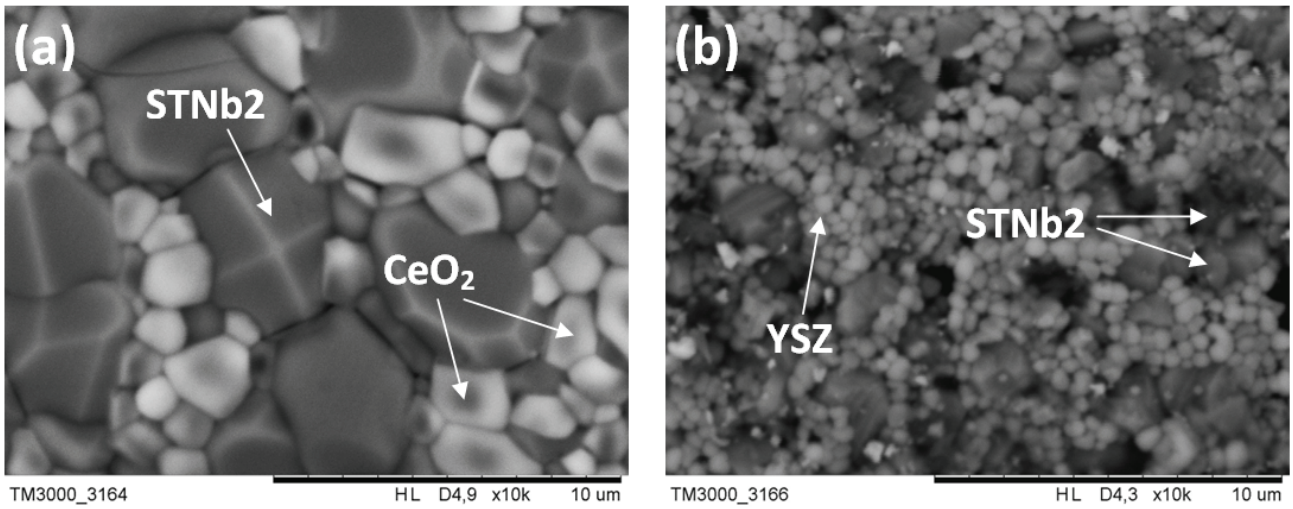

Figure 1. SEM images of the cross-sections of composite bulk samples: a) 70STNb2-30CeO_2 and b) 70STNb2-30YSZ reduced at 1400 °C for 10 h in H_2

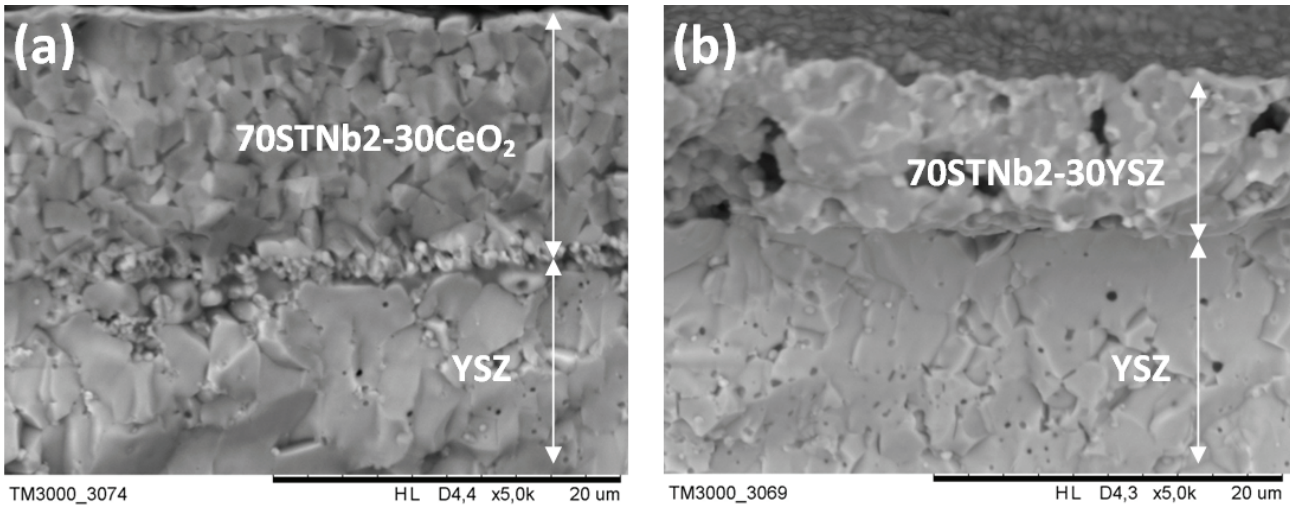

Figure 2. SEM images of the cross-sections of half-cells with different anodes: a) 70STNb2-30CeO_2 and b) 70STNb2-30YSZ reduced at 1400 °C for 10 h in H_2

temperature reduction in hydrogen. This mechanical instability increases with ceria content in the composite. Simultaneously, the composites containing YSZ remain mechanically stable during redox cycles. Koutcheiko *et al.* [8] reported that this cracking of composite with CeO_2 is caused by the contraction of the CeO_2 lattice parameter in less reducing atmospheres. In air the thermal expansion coefficient (TEC) of composites consisting of Y-doped $SrTiO_3$ and CeO_2 is very similar to the TEC of YSZ [8]. However, TEC increases in a reducing atmosphere and changes with CeO_2 content in the composite [8,13]. The more ceria forms grains at grain boundaries, the easier the bulk pellets crack. This TEC mismatch in low oxygen partial pressure results also in the delamination of composite layers from the YSZ electrolyte support.

The cross-sectional images of the composites applied as porous layers at the STNb2-YSZ/YSZ and STNb2-CeO_2/YSZ interfaces, are presented in Fig. 2. There is a significant difference in morphology of the investigated porous layers. The 70STNb2-30CeO_2 layer seems to be almost dense, whereas in 70STNb2-30YSZ large (up to 2 μm) and quite randomly distributed pores are visible. Also the interface between anode and electrolyte differs significantly. In the case of the composite thick film with YSZ there is a clear boundary between anode and electrolyte phases and there are some holes at the interface. On the other hand, at the interface between 70STNb2-30CeO_2 and electrolyte a presence of fine-crystalline material can be observed. We suggest that it may be ceria that had diffused from the composite interior. Thus, the interface between anode and electrolyte seems to be the most energetically favourable for ceria diffusion. In Fig. 3 we can see the surface of both composite anodes used in the half cells. In contradiction to the surface of the 70STNb2-30YSZ composite (Fig. 3b), in which grains of both phases have a similar size (1 μm) and are well distributed, on the surface of the 70STNb2-30CeO_2 composite (Fig. 3a) we can find mostly large, elongated crystallites (up to 10 μm). The

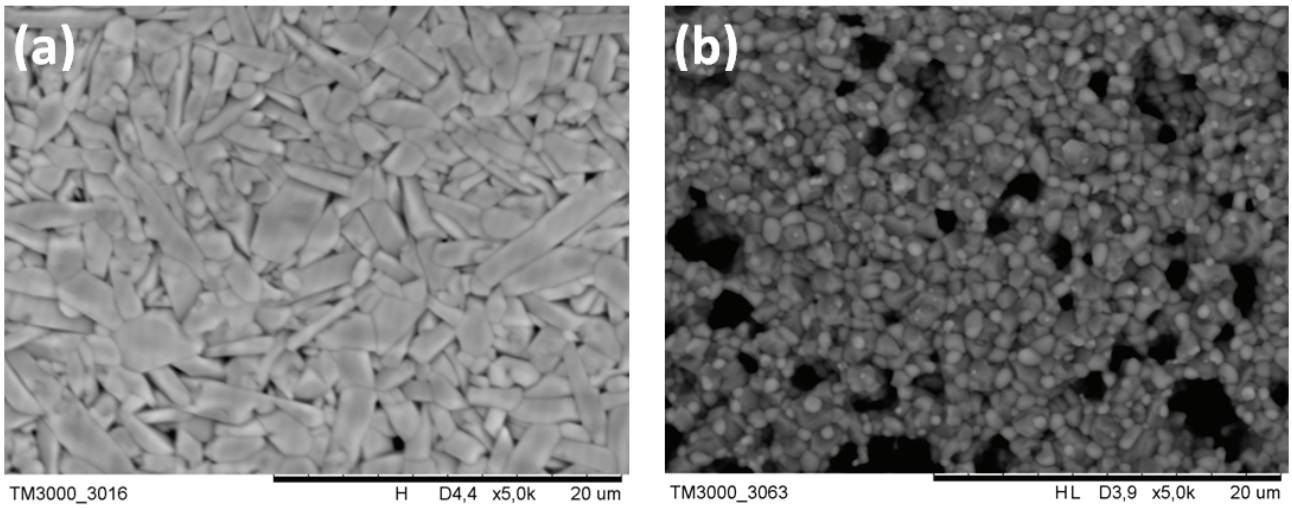

Figure 3. SEM images of the surface of half-cells with different anodes: a) 70STNb2-30CeO_2 and b) 70STNb2-30YSZ reduced at 1400 °C for 10 h in H_2

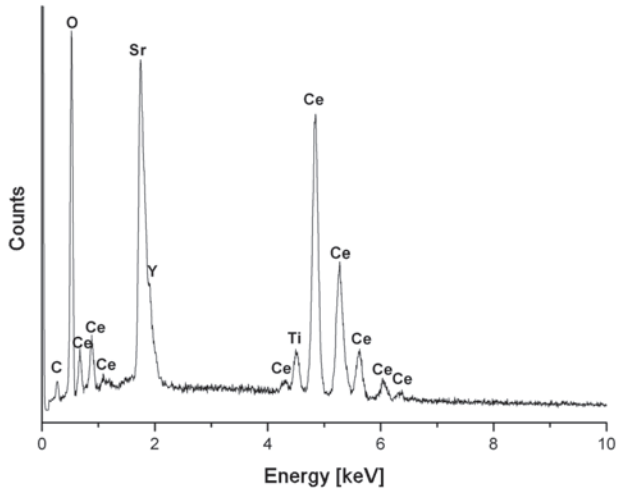

Figure 4. EDX spectrum of the surface of half-cell with 70STNb2-30CeO_2 anode shown in Fig. 3a

EDX technique was used to identify these grains. The result of EDX analysis performed on the surface of the half-cell with 70STNb2-30CeO_2 anode n order to identify these grains (Fig. 3a) is presented in Fig. 4. It can be concluded that the dominant element in the analyzed layer is cerium. The weight amount of cerium was recognized as almost three times higher than strontium. As the SEM image (Fig. 3a) indicates that the surface layer consists of a single-phase, the presence of strontium can be explained by the specification of the EDX measurements in which elements even up to 2 μm below the analyzed surface can be detected. That is the reason why, when using the EDX method, we can identify not only a large amount of ceria on the surface but also composite components below this 1 μm thick ceria layer. Observations made after the using EDX technique confirm previous suggestions that ceria diffuses to the surface from the interior of the composite as it was observed at the anode/electrolyte interface as well.

Results of the electrical conductivity measurements performed at the composite bulk samples and porous composite layers are presented in Fig. 5a,b. Both analyzed bulk composites show conductivity higher than 1 S/cm that is required to minimize the anode ohmic losses if the material is used for solid oxide fuel cell [14]. Although a conductivity of the bulk 85STNb2-15CeO_2 (Fig. 5a) is lower than that of 85STNb2-15YSZ (Fig. 5b), it does not change a lot when the former composition is applied as porous layer. In contrast, conductivity of the porous 85STNb2-15YSZ (Fig. 5b) is two orders of magnitude lower than in the case of the bulk sample. It reveals an advantage of 85STNb2-15CeO_2 over the 85STNb2-15YSZ in relation to bulk samples that can be explained by many factors.

Firstly, composite with CeO_2 forms an almost dense layer, whereas in the composite with YSZ large (up to 2 μm) and quite randomly distributed pores are visible, as was shown in Fig. 2a,b. However, the observed densification of composite layer with CeO_2 is an undesired phenomenon, because if it is applied in an operating fuel cell, it decreases the triple phase boundary and deteriorates the gas exchange on the anode's side.

Secondly, the lower conductivity of the 85STNb2-15YSZ layer than that of the bulk sample can be explained by the Ti diffusion from STNb2 phase. It has been reported [9,12] that titanium can migrate to the YSZ. Composite material that is depleted with Ti has lower conductivity than the initial composition. We have previously observed [15] that the diffusion of Ti to YSZ support is limited in composite layers containing CeO_2, which may explain their higher conductivity compared to the composites with YSZ.

Finally, the higher conductivity of 85STNb2-15CeO_2 layer than that of 85STNb2-15YSZ in relation to bulk samples can be explained by the fact that ceria exhibits high electronic conductivity after reduction [16]. As it

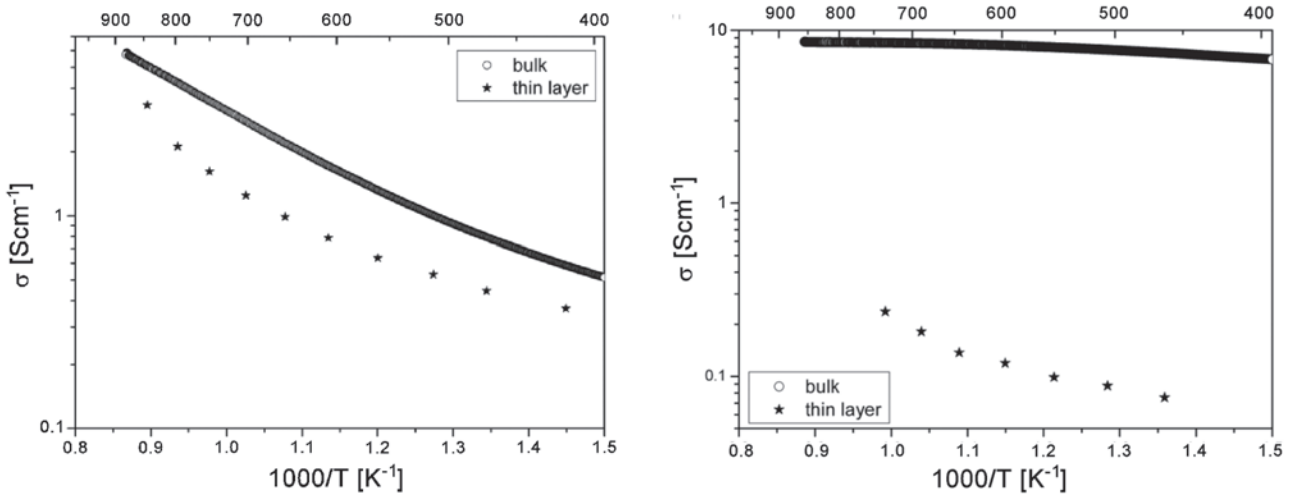

Figure 5. The comparison of electrical conductivity plots of: a) 85STNb2-15CeO_2 and b) 85STNb2-15YSZ bulk samples (reduced at 1400 °C for 10 h in H_2) vs. thin layers as a function of temperature

was observed in Figs. 2a and 3a and confirmed by EDX spectrum shown in Fig. 4, there is a dense layer consisting mostly of ceria. This surface layer after reduction may have much higher conductivity than the interior of composite that can result in the decrease of 85STNb2-15CeO_2 resistance compared to 85STNb2-15YSZ.

IV. Conclusions

It was observed that CeO_2 in the composite has a tendency to accumulate in more energetically favourable areas. In bulk samples this process was observed at the grain boundaries, whereas in porous layers it was seen at the surface and at the anode/electrolyte interface. It resulted in the lower samples resistance to cracking and layers delamination from the YSZ electrolyte substrate. Although the total electrical conductivity of layer with CeO_2 was higher than that with YSZ, it could not improve the properties of the fuel cell when applied as an anode. The observed densification of ceria containing layer reduced the triple phase boundary and deteriorated the gas exchange on the anode's side. In consequence, the overall performance of the operating fuel cell could be lower.

It can be concluded that STNb2-YSZ composite seems to have better properties than STNb2-CeO_2 and can be applied as anode or anode/electrolyte interface layer for SOFC.

Acknowledgements: This work was supported by the National Science Center under the grant No. NCN DEC-2011/01/N/ST5/05579. Authors would also like to acknowledge A. Krupa and J. Karczewski for help in measurements and valuable comments on the obtained results.

References

1. J.W. Fergus, "Oxide anode materials for SOFC", *Solid State Ionics*, **177** (2006) 1529–1541.
2. W.Z. Zhu, S.C. Deevi, "A review on the status of anode materials for SOFC", *Mater. Sci. Eng. A*, **362** (2003) 228–239.
3. Y. Matsuzaki, I. Yasuda, "The poisoning effect of sulfur-containing impurity gas on a SOFC anode: Part I. Dependence on temperature, time, and impurity concentration", *Solid State Ionics*, **132** (2000) 261–269.
4. R. Astala, P.D. Bristowe, "Ab initio and classical simulations of defects in $SrTiO_3$", *Comput. Mater. Sci.*, **22** (2001) 81–86.
5. J. Karczewski, B. Riegel, M. Gazda, P. Jasinski, B. Kusz, "Electrical and structural properties of Nb-doped $SrTiO_3$ ceramics", *J. Electroceram.*, **24** (2010) 326–330.
6. Q. Ma, F. Tietz, A. Leonide, E. Ivers-Tiffée, "Electrochemical performances of solid oxide fuel cells based on Y-substituted $SrTiO_3$ ceramic anode materials", *J. Power Sources*, **196** (2011) 7308–7312.
7. P. Blennow, A. Hagen, K.K. Hansen, L.R. Wallenberg, M. Mogensen, "Defect and electrical transport properties of Nb-doped $SrTiO_3$", *Solid State Ionics*, **179** (2008) 2047–2058.
8. S. Koutcheiko, Y. Yoo, A. Petric, I. Davidson, "Effect of ceria on properties of yttrium-doped strontium titanate ceramics", *Ceram. Int.*, **32** (2006) 67–72.
9. Q. Ma, F. Tietz, D. Sebold, D. Stöver, "Y-substituted $SrTiO_3$-YSZ composites as anode materials for solid oxide fuel cells: Interaction between SYT and YSZ", *J. Power Sources*, **195** (2010) 1920–1925.
10. M.D. Gross, K.M. Carver, M.A. Deighan, A. Schenkel, B.M. Smith, A.Z. Yee, "Redox stability of $SrNb_xTi_{1-x}O_3$-YSZ for use in SOFC anodes", *J. Electrochem. Soc.*, **156** [4] (2009) B540–B545.
11. X. Sun, S. Wang, Z. Wang, J. Qian, T. Wen, F. Huang, "Evaluation of $Sr_{0.88}Y_{0.08}TiO_3$-CeO_2 as composite anode for solid oxide fuel cells running on CH_4 fuel", *J. Power Sources*, **187** (2009) 85–89.
12. B. Bochentyn, J. Karczewski, S. Molin, T. Klimczuk, M. Gazda, P. Jasinski, D.J. Safarik, B. Kusz, "The comparison of $SrTi_{0.98}Nb_{0.02}O_{3-\delta}$-$CeO_2$ and $SrTi_{0.98}Nb_{0.02}O_{3-\delta}$-YSZ composites for use in SOFC anodes", *J. Electroceram.*, DOI 10.1007/s10832-012-9693-8.
13. M. Mogensen, N.M. Sammes, G.A. Tompsett, "Physical, chemical and electrochemical properties of pure and doped ceria", *Solid State Ionics*, **129** (2000) 63–94.
14. S. Tao, J.T.S. Irvine, "Synthesis and characterization of $(La_{0.75}Sr_{0.25})Cr_{0.5}Mn_{0.5}O_{3-\delta}$, a redox-stable, efficient perovskite anode for SOFCs", *J. Electrochem. Soc.*, **151** (2004) A252–A259.
15. B. Bochentyn, J. Karczewski, S. Molin, M. Gazda, P. Jasinski, B. Kusz, "Characterization of composite materials based of Nb-doped strontium titanate: Interactions between phases", *Solid State Ionics*, 2012, submitted.
16. G. Kim, J.M. Vohs, R.J. Gorte, "Enhanced reducibility of ceria-YSZ composites in solid oxide electrodes", *J. Mater. Chem.*, **18** (2008) 2386–2390.